ACS Macro Letters

Letter

pubs.acs.org/macroletters

Shift-Time Polyelectrolyte Multilayer Assembly: Fast Film Growth and High Gas Barrier with Fewer Layers by Adjusting Deposition Time

David A. Hagen, Brendan Foster, Bart Stevens, and Jaime C. Grunlan*

Department of Mechanical Engineering, Texas A&M University, College Station, Texas 77843, United States

ABSTRACT: In an effort to reduce deposition time and number of layers needed to achieve high gas barrier, multilayer films were deposited using 1 s exposures for the first four bilayers (BLs) and 1 min for subsequent dips. Thin-film assemblies of polyethylenimine (PEI) and poly(acrylic acid) (PAA) were deposited onto poly(ethylene terephthalate) [PET] using the layer-by-layer deposition process. Varying the exposure time of PET to polyelectrolyte solutions (i.e., dip time) significantly alters the growth rate of the multilayer thin films. The PEI/PAA system grows linearly with 1 s dip times and exponentially with longer times. Eight bilayers (650 nm) were required to achieve an undetectable oxygen transmission rate (<0.005 $cm^3/(m^2 \cdot day)$) using 1 min deposition steps, but this barrier was obtained with only 6 BLs (552 nm) using 1s deposition of the initial layers, reducing total deposition time by 73%. This "shift-time" concept makes layer-by-layer assembly much faster and more commercially feasible.

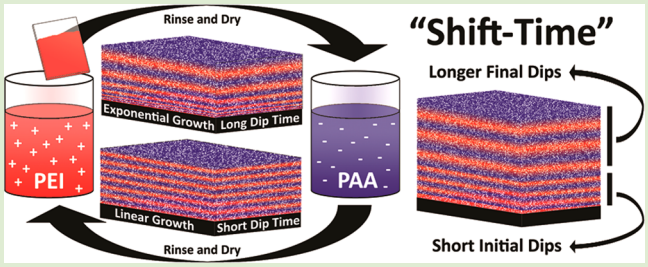

Layer-by-layer (LbL) deposition is a technique used to precisely deposit nanostructured thin films that can exhibit exceptional properties. Alternately depositing materials with complementary functionalities, such as opposite electrostatic charges, allows for controlled thin-film growth.[1] Many types of materials can be used to construct these films, including polymers,[2] nanosheets,[3] nanotubes,[4] quantum dots,[5] and biological molecules.[6] There are many parameters that affect the interactions between these components such as molecular weight,[7] pH, ionic strength, concentration,[8] and deposition time,[9−11] which consequently alter the thickness, morphology, and properties of the multilayer thin film. Tailoring these interactions allows for the design of assemblies that exhibit desirable properties. LbL assembled films have been engineered to deliver drugs,[12] impart electrical conductivity,[13] reduce gas permeability,[14−17] resist abrasion,[18] kill bacteria,[19] separate gases,[20] and stop fire.[21,22]

Flexible gas barrier thin films are of particular interest for food packaging, pressurized systems, and flexible electronics encapsulation.[23−25] The metalized plastic film used for food packaging suffers from cracking and the inability to be microwaved, which could be solved by using LbL thin films. There are potential benefits of using lightweight gas barrier films in various pressurized systems like sporting goods and aircraft. Flexible electronic displays require a good gas barrier to protect the underlying components from oxidative degradation.

When considering the implementation of layer-by-layer technology for these applications, the adage "time is money" holds true. In this case, it could be said that *processing time* is money. Layer-by-layer has traditionally been a slow process, with deposition times per layer ranging from 30 s to 25 min.[8,26−29] Faster methods for deposition include spraying[29−31] and spin coating,[32] but traditional immersion (or dipping) remains a viable option if shorter deposition times and fewer layers can be used. In an effort to reduce processing time, the "shift-time" method was developed to reduce the number of layers needed to achieve a desired property and reduce the exposure time for each layer. By reducing the processing time of initial layers, a sufficient film thickness to attain an undetectable oxygen barrier was constructed with fewer layers. This novel approach is illustrated in Figure 1.

The polyethylenimine (PEI)/poly(acrylic acid) (PAA) system has been shown to grow exponentially with 1 min dips when PEI is at pH 10 and PAA is at pH 4.[33] Each polymer is weakly charged at these pH levels, causing the polymer chains to assume a globular conformation due to minimal self-repulsion. For the deposition of PAA onto a PEI-covered surface, the deposited PEI becomes highly charged in the pH 4 PAA solution, which requires more PAA to deposit to satisfy this charge. Likewise, the PAA surface also becomes highly charged in the alternate solution, causing more PEI to deposit. The complementary nature of these pH conditions allows for exponential growth. Eight PEI/PAA bilayers, deposited on a 175 μm PET substrate, are 651 nm thick and exhibit an undetectable oxygen transmission rate (OTR <0.005 $cm^3/(m^2 \cdot day)$), which is 3 orders of magnitude lower than uncoated PET.[33]

Received: May 9, 2014
Accepted: June 16, 2014
Published: June 19, 2014

   dx.doi.org/10.1021/mz500276r | *ACS Macro Lett.* 2014, 3, 663−666

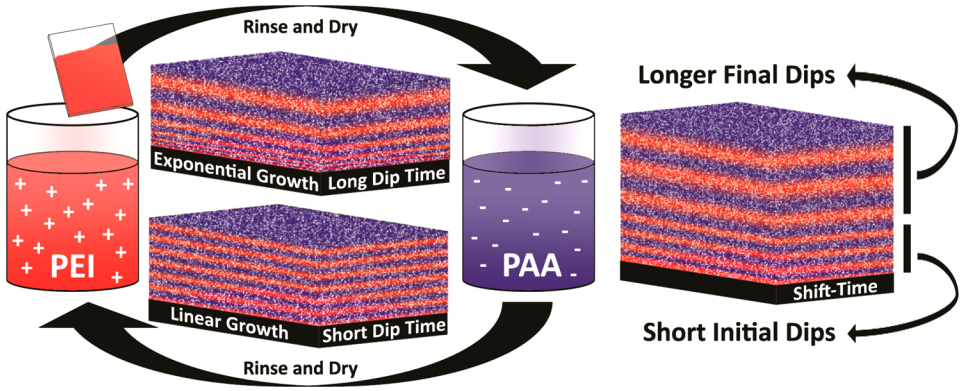

Figure 1. Schematic of the shift-time layer-by-layer dipping process used to achieve thicker films, with fewer layers, without altering the ingredients used.

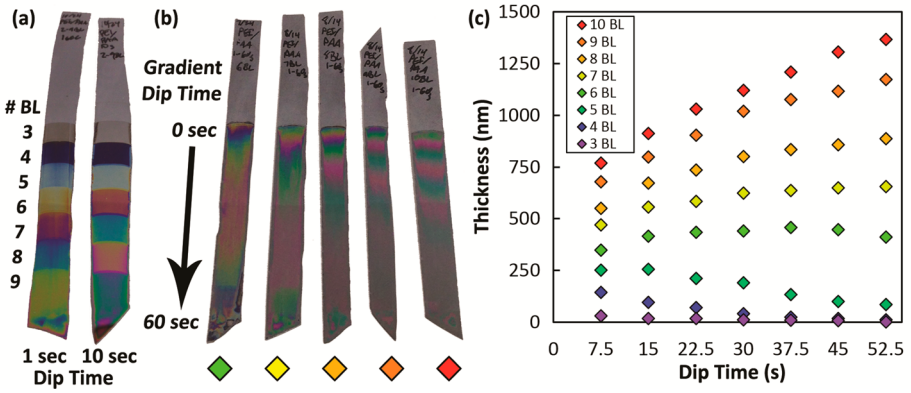

Figure 2. Images of PEI/PAA thin-film assemblies on silicon wafers with (a) different dip times for each wafer and stripes of different bilayers and (b) wafers of different numbers of bilayers with a gradient of dip time. (c) Profilometer thickness of gradient wafers at different numbers of bilayers. Colored diamonds in (b) correspond to the same colors in (c). These thickness data were acquired with profilometry.

The influence of dip time on the growth of PEI/PAA assemblies was evaluated using a robotic system that dipped the entire substrate for the first *n* bilayers and then lessened the submersion depth incrementally for each successive bilayer.[34] This procedure created 6 mm stripes that allowed measurement of thickness as a function of bilayers deposited, as shown in Figure 2(a). The colors observed on the silicon wafers are the result of constructive interference of the light reflecting off the film surface and underlying silicon surface, where different colors indicate different thickness. To examine the influence of a continuous range of dip times (0−60 s), a deposition time gradient was generated along a single wafer by submerging and removing the entire wafer at a given speed, as shown in Figure 2(b). The thickness data from these wafers show that longer dip times create thicker films, which agrees with previous work where it was shown that the growth rate (i.e., thickness change per bilayer) is a result of the time-dependent polymer diffusion process.[26,30,35] It should be noted that before these films reach a critical thickness, shorter dip times lead to thicker growth. These polymers deposit as coils, but as the films are held in solution some polymer chains are rejected from the surface. The remaining chains flatten onto the surface, obtaining a more thermodynamically stable conformation with more of the charged groups paired with surface charges.[36] As layers are deposited, diffusion into the film allows for much thicker deposition, but the relaxation phenomenon causes the longer dip times to have a very slow initial growth period. For exponentially growing LbL films, the growth rate increases as bilayers are deposited due to the additional amount of underlying film into which the polymer can diffuse. When the film no longer becomes saturated at a given deposition time, the growth transitions from exponential to linear. The final linear growth rate is diffusion limited, with longer depositions providing larger growth rates.[26] For the films deposited in shorter intervals, there is almost no transition, and the final linear growth is obtained after only three bilayers. These films have the highest growth rate for the first few bilayers due to a limited time for chain relaxation, leaving a thick tightly coiled layer. Although they reach this final linear growth regime with the fewest number of BLs, the shorter dip time films have the smallest final growth rate due to limited diffusion of polymer into the underlying film.

The shift-time method takes advantage of the high initial growth rate of the short deposition time and the high linear growth of the longer deposition time by initiating the film growth with a short dip time and then transitioning to a longer dip time. Exposures of 1 s and 1 min are used because these correspond to the extrema of the trends observed within this time domain. The first four bilayers were deposited with 1 s dips to quickly build enough material to support the full diffusion of 1 min dips. Figure 3 shows that the growth rate of the shift-time film (260 nm/BL), during 1 min dips, nearly matches that of the film that was constructed entirely with 1 min dips (280 nm/BL), but shift-time achieved a similar thickness with two fewer bilayers, 650 nm at 8 BL and 552 nm at 6 BL, respectively. Furthermore, the total deposition time for

dx.doi.org/10.1021/mz500276r | *ACS Macro Lett.* 2014, 3, 663−666

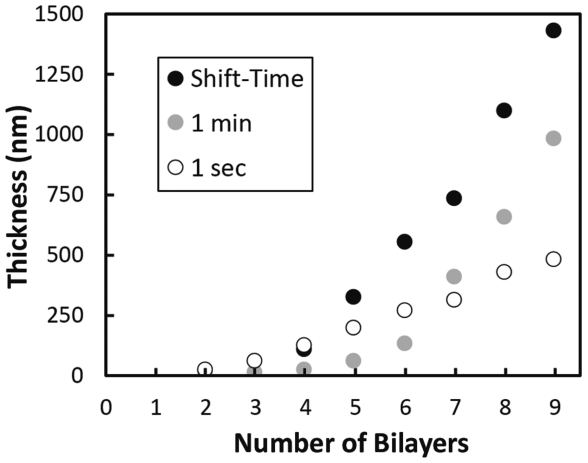

Figure 3. Thickness as a function of PEI/PAA bilayers deposited with 1 min, 1 s, and shift-time depositions, where the first four BLs of the shift-time film are 1 s and the succeding layers are 1 min. These thickness data were acquired with ellipsometry.

eight bilayers with 1 min dips is 16 min, while a 6 BL shift-time assembly, having comparable thickness, reduced deposition time to approximately 4 min.

Figure 4 shows oxygen transmission rate as a function of bilayers deposited. The films deposited with 1 s dips show an

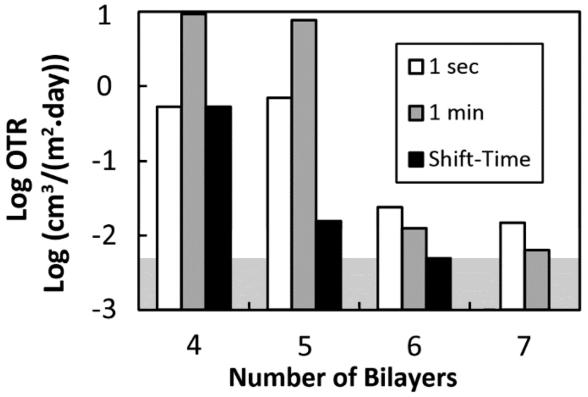

Figure 4. Oxygen transmission rate as a function of PEI/PAA bilayers deposited with 1 min, 1 s, and shift-time dips, where the first four BLs of the shift-time film are 1 s and the succeeding layers are 1 min. The shaded background represents the undetectable range of OTR testing equipment (<0.005 $cm^3/(m^2 \cdot day)$).

order of magnitude improvement over the bare PET substrate at four bilayers, while the films produced with 1 min deposition showed relatively little improvement due to the thin growth through five bilayers. The shift-time film shows a significant improvement in barrier performance from the fourth to the fifth bilayer, which is its first 1 min deposition BL. Only shift-time assemblies achieve the undetectable OTR limit of 0.005 $cm^3/(m^2 \cdot day)$ at 6 BL, which is more than 3 orders of magnitude lower than over the 179 μm PET substrate. This 552 nm thick film exhibits the greatest oxygen barrier reported in the literature for a LbL film composed of 12 (or fewer) total layers (i.e., 6 BL). In many cases, the OTR achieved with five bilayers (0.016 $cm^3/(m^2 \cdot day)$) would be enough for many packaging applications and could be deposited roll-to-roll with a flexographic or multilayer slot printer.[37]

EXPERIMENTAL SECTION

Poly(acrylic acid) (PAA) (M_w = 100 000 g/mol, ρ = 1.20 g/cm^3), purchased from Sigma-Aldrich (Milwaukee, WI), was used as a 0.2 wt % solution in DI water and adjusted to pH 4.0 using 1 M NaOH. Branched polyethylenimine (PEI) (M_w = 25 000 g/mol, ρ = 1.10 g/cm^3) was also purchased from Sigma-Aldrich and used as a 0.1 wt % DI water solution, adjusted to pH 10.0 using 1 M HCl.

Poly(ethylene terephthalate) (PET) film, with a thickness of 179 μm (trade name ST505, produced by Dupont-Teijin), was purchased from Tekra (New Berlin, WI) and used as the substrate for oxygen transmission rate testing. This PET film has an OTR of approximately 9 $cm^3/(m^2 \cdot day \cdot atm)$ under dry conditions. Prior to deposition, PET substrates were rinsed with methanol and DI water, followed by treatment of each side of the substrate using a BD-20C Corona Treater (Electro-Technic Products, Inc., Chicago) to ensure an adequate negative surface charge. Polished silicon wafers were purchased from University Wafer (South Boston, MA) and were used as substrates for ellipsometry and profilometry. They were treated with piranha solution in a 3:1 mass ratio of 30% hydrogen peroxide to 99% sulfuric acid and stored in deionized (DI) water [*Caution! Piranha solution should be handled with extreme caution!*]. Silicon wafers were rinsed with acetone and DI water prior to deposition.

Each substrate was dipped into the cationic PEI solution for the designated dip time (i.e., 1 s or 1 min). After this, and every subsequent dip, the substrate was pulled through a curtain of DI water at a speed of 25 mm/s to rinse off excess solution and then similarly dried with filtered air at a speed of 2.5 mm/s. The total time between each solution immersion was approximately 1 min. The substrate was then dipped into the anionic PAA solution for the same duration, which completed a single bilayer dipping cycle, as illustrated in Figure 1. For gradient deposition, 51 mm wafer sections were submerged into and immediately removed from solutions at a speed of 102 mm/min, so the resulting films were deposited with a linear gradient of dip times (0 to 1 min) along the wafer (Figure 2(b)). This method demonstrates the thickness trends, but actual thickness values referenced in the text are taken from discrete wafers shown in Figure 2(a), which were constructed in the same manner as the films tested for OTR.

Thickness measurements were taken as a function of layers deposited using an α-SE spectroscopic ellipsometer (J.A. Woodlam Co., Inc., Lincoln, NE). For the gradient films, thickness was measured with a $P\bar{6}$ profilometer (KLA-Tencor, Milpitas, CA). Multiple scratches were made at each position so that height from the leveled substrate could be taken. All thickness values reported are an average of three measurements, and growth rates were calculated using linear regression. OTR testing was performed according to ASTM D-3985 specifications by MOCON (Minneapolis, MN) using an Oxtran 2/21 ML instrument at testing conditions of 23 °C and 0% RH.

AUTHOR INFORMATION

Corresponding Author

*E-mail: jgrunlan@tamu.edu.

Notes

The authors declare no competing financial interest.

ACKNOWLEDGMENTS

The authors acknowledge The Dow Chemical Company and the Texas A&M Engineering Experiment Station for financial support of this work.

REFERENCES

(1) Decher, G.; Schlenoff, J. B. *Multilayer Thin Films*; Wiley-VCH Verlag GmbH & Co. KGaA: Weinheim, Germany, 2012.
(2) Lee, S. W.; Lee, D. *Macromolecules* **2013**, *46*, 2793−2799.
(3) Yang, Y.-H.; Bolling, L.; Priolo, M. A.; Grunlan, J. C. *Adv. Mater.* **2013**, *25*, 503−508.
(4) Pan, Y.; Zhang, Y.-Z.; Li, Y. *J. Appl. Polym. Sci.* **2013**, *128*, 647−652.

(5) Xiao, F. X.; Miao, J. W.; Liu, B. *J. Am. Chem. Soc.* **2014**, *136*, 1559−1569.
(6) Deng, Z. J.; Morton, S. W.; Ben-Akiva, E.; Dreaden, E. C.; Shopsowitz, K. E.; Hammond, P. T. *ACS Nano* **2013**, *7*, 9571−9584.
(7) Porcel, C.; Lavalle, P.; Decher, G.; Senger, B.; Voegel, J. C.; Schaaf, P. *Langmuir* **2007**, *23*, 1898−1904.
(8) Ferreira, M.; Rubner, M. F. *Macromolecules* **1995**, *28*, 7107−7114.
(9) Yang, Y.-H.; Malek, F. A.; Grunlan, J. C. *Ind. Eng. Chem. Res.* **2010**, *49*, 8501−8509.
(10) Xiang, F.; Tzeng, P.; Sawyer, J. S.; Regev, O.; Grunlan, J. C. *ACS Appl. Mater. Interfaces* **2014**, *6*, 6040−6048.
(11) Mermut, O.; Barrett, C. J. *J. Phys. Chem. B* **2003**, *107*, 2525−2530.
(12) Min, J.; Braatz, R. D.; Hammond, P. T. *Biomaterials* **2014**, *35*, 2507−2517.
(13) Yu, B.; Liu, X. M.; Cong, H. L.; Wang, Z. H.; Tang, J. G. *Sci. Adv. Mater.* **2013**, *5*, 1533−1538.
(14) Rajasekar, R.; Kim, N. H.; Jung, D.; Kuila, T.; Lim, J. K.; Park, M. J.; Lee, J. H. *Compos. Sci. Technol.* **2013**, *89*, 167−174.
(15) Tzeng, P.; Maupin, C. R.; Grunlan, J. C. *J. Membr. Sci.* **2014**, *452*, 46−53.
(16) Gokhale, A. A.; Lu, J.; Parker, N. J.; Izbicki, A. P.; Sanyal, O.; Lee, I. *J. Colloid Interface Sci.* **2013**, *409*, 219−226.
(17) Priolo, M. A.; Gamboa, D.; Holder, K. M.; Grunlan, J. C. *Nano Lett.* **2010**, *10*, 4970−4974.
(18) Qureshi, S. S.; Zheng, Z. Q.; Sarwar, M. I.; Felix, O.; Decher, G. *ACS Nano* **2013**, *7*, 9336−9344.
(19) Iarikov, D. D.; Kargar, M.; Sahari, A.; Russel, L.; Gause, K. T.; Behkam, B.; Ducker, W. A. *Biomacromolecules* **2014**, *15*, 169−176.
(20) Kim, D.; Tzeng, P.; Barnett, K. J.; Yang, Y.-H.; Wilhite, B. A.; Grunlan, J. C. *Adv. Mater.* **2014**, *26*, 746−751.
(21) Laufer, G.; Kirkland, C.; Morgan, A. B.; Grunlan, J. C. *ACS Macro Lett.* **2013**, *2*, 361−365.
(22) Carosio, F.; Di Blasio, A.; Cuttica, F.; Alongi, J.; Frache, A.; Malucelli, G. *Ind. Eng. Chem. Res.* **2013**, *52*, 9544−9550.
(23) Graff, G. L.; Burrows, P. E.; Williford, R. E.; Praino, R. F. Barrier Layer Technology for Flexible Displays. In *Flexible Flat Panel Displays*; John Wiley & Sons, Ltd.: Chichester, UK, 2005; pp 57−77.
(24) Bowles, M.; Jianjun, L. In Review on nanotechnology in agricultural products logistics management, *8th International Conference on Computing and Networking Technology (ICCNT)*, 27−29 Aug. 2012; pp 415−420.
(25) Yam, K. L.; Lee, D. S. *Emerging food packaging technologies: Principles and practice*; Woodhead Publishing: Cambridge, UK, 2012.
(26) Podsiadlo, P.; Michel, M.; Lee, J.; Verploegen, E.; Kam, N. W. S.; Ball, V.; Lee, J.; Qi, Y.; Hart, A. J.; Hammond, P. T.; Kotov, N. A. *Nano Lett.* **2008**, *8*, 1762−1770.
(27) Lvov, Y.; Decher, G.; Moehwald, H. *Langmuir* **1993**, *9*, 481−486.
(28) Lvov, Y.; Ariga, K.; Ichinose, I.; Kunitake, T. *J. Am. Chem. Soc.* **1995**, *117*, 6117−6123.
(29) Izquierdo, A.; Ono, S. S.; Voegel, J. C.; Schaaf, P.; Decher, G. *Langmuir* **2005**, *21*, 7558−7567.
(30) Porcel, C.; Lavalle, P.; Ball, V.; Decher, G.; Senger, B.; Voegel, J.-C.; Schaaf, P. *Langmuir* **2006**, *22*, 4376−4383.
(31) Saetia, K.; Schnorr, J. M.; Mannarino, M. M.; Kim, S. Y.; Rutledge, G. C.; Swager, T. M.; Hammond, P. T. *Adv. Funct. Mater.* **2014**, *24*, 492−502.
(32) Habazaki, H.; Kimura, T.; Aoki, Y.; Tsuji, E.; Yano, T. *J. Electrochem. Soc.* **2014**, *161*, C57−C61.
(33) Yang, Y.-H.; Haile, M.; Park, Y. T.; Malek, F. A.; Grunlan, J. C. *Macromolecules* **2011**, *44*, 1450−1459.
(34) Jang, W.-S.; Grunlan, J. C. *Rev. Sci. Instrum.* **2005**, 76.
(35) Bieker, P.; Schönhoff, M. *Macromolecules* **2010**, *43*, 5052−5059.
(36) McAloney, R. A.; Goh, M. C. *J. Phys. Chem. B* **1999**, *103*, 10729−10732.
(37) Krebs, F. C. *Sol. Energy Mater. Sol. Cells* **2009**, *93*, 394−412.